

AEROELASTIC ANALYSIS OF HELICOPTER ROTOR BLADE WITH ADVANCED TIPS AND TRAILING EDGE FLAPS

Wei-Dong Yang Cheng-Lin Zhang Shi-Cun Wang

Research Institute of Helicopter Technology,
Nanjing University of Aeronautics and Astronautics,
Nanjing 210016, China

Abstract

A comprehensive aeroelastic analysis of helicopter rotor blade with advanced tips and trailing edge flaps is coupled with a unsteady aerodynamic model and a efficient rotor wake modeling. The aeroelastic analysis is based on finite element theory in space and time. Each rotor blade is assumed to undergo flap bending, lag bending and elastic twist deflections. The blade response is calculated from nonlinear periodic equations using a finite element in time scheme. An unsteady aerodynamic model including flap effects is used for calculating the airloads of two dimensional airfoil with trailing edge flap. For induced inflow distributions on the rotor disk, a constant vorticity contour wake model is used. Numerical results show that blade response and loads are sensitive to wake model, tip sweep angle and trailing edge flap. The rotor wake analysis is important for capturing the harmonics of low speed aerodynamic loads. The swept tip increases the vibratory component of torsional loads. The trailing edge flap inputs increase the blade torsional response as compared to the baseline blade.

h	plunge displacement (positive down)
k	reduced frequency
l_{tip}	swept tip length
L_u, L_v, L_w	aerodynamic loads distributed along length of blade in axial, lag and flap directions, respectively
M_ϕ	aerodynamic moment in torsional direction
M_y	flap bending moment at blade root
\vec{r}_b, \vec{r}'_b	position vectors of point P before and after deformations
R	rotor radius
T_{mn}	transformation matrix relating n-th to m-th segment coordinates
\vec{V}_b	velocity of point P in local coordinate
$\delta U, \delta V, \delta W$	variations in the strain energy, the kinetic energy and the virtual work done by external forces respectively
u, v, w	blade elastic displacements in the axial, lag and flap directions
x, η, ζ	curvilinear coordinates
α	angle of attack
α_s, ϕ_s	attack angles of rotor disk
δ	flap deflection angle
γ	Lock number
λ	rotor inflow ratio
μ	rotor advance ratio
$\theta_0, \theta_{1c}, \theta_{1s}$	pitch control settings
θ_p	blade pitch
θ_{tw}	blade pretwist
ρ	mass density of beam
σ	solidity ratio
Ω	angular velocity of rotor

Nomenclature

a	pitch axils location (semi-chords)
b	semichord
$C(k)$	Theodorsen's function
C_M	moment coefficient about 1/4-chord
C_N	lift force coefficient
C_W	weight coefficient
e	flap hinge location (semi-chords)
\vec{e}_{tr}	hub-fixed rotating coordinates system
$F_1 - F_{20}$	geometric constants for flap
F_z	vertical shear force at blade root

Subscripts

$(\)_r$ refers to quasi-steady

θ_{tip} refers to blade tip

Introduction

Helicopter rotors operating in high speed flight encounter transonic flow conditions on the advancing blade tips. A drag rise associated with the transonic flow increases the power needed to drive the rotor, and the vibration levels associated with the high speed flight condition increases considerably. One way to reduce the drag rise on the advancing side is to modify the tip planform of the blade. To reduce the vibration levels, one can use the active control technology. With the development and application of composite materials and advanced smart structures, the feasibility of using advanced tips and trailing edge flaps has increased substantially for improving helicopter rotor performance and reducing vibration levels.

Early research on swept-tip blades was primarily focused on aerodynamic performance characteristics of blades (Ref 1-2). Desoer performed aerodynamic calculations of an isolated rigid blade with advanced tips using a detailed CFD method (Ref 1). Celi and Friedmann used a Galerkin type finite element approach to refine the structural representation of swept-tip blade, and studied the aeroelastic response and stability of the rotor in forward flight (Ref 3). Benquet and Chopra developed an aeroelastic formulation for the advanced tip using the finite element method based on Hamilton's principle (Ref 4). Kim developed the formulation to include nonlinear transformation relations between the tip and the main inboard blade. Three-dimensional aerodynamics was also included (Ref 5). Bir and Chopra developed a new formulation restricted not to blade tip alone but applicable to a blade varying sweep, droop, twist and planform. The effects of fuselage motion in formulation of forces were also included (Ref 6).

Vibration reduction with trailing edge flaps has been the subject of several experimental and analytical studies in recent years (Ref 7-9). These studies involved plain trailing edge flaps. Such flaps are hinged portions of the individual blade and are used for lift control. Another type of flaps, the servo flaps, are mounted aft of the blade trailing edge, and thus provide

substantial pitching moments as well as changing airfoil lift characteristics. Millott and Friedmann implemented a feasibility study utilizing a spring-restrained offset-hinged rigid blade (Ref 10), and then, the analysis was improved to include an elastic blade model, refinements to the aerodynamic model, and a time domain solution (Ref 11-12).

In the present study, a comprehensive aeroelastic analysis of helicopter rotor blade with advanced tips and trailing edge flaps is coupled with a unsteady aerodynamic model and a efficient rotor wake modeling. The aeroelastic analysis is based on finite element theory in space and time. In order to better represent the structural modeling of the advanced tip, a special finite element is developed to model the tip of blade. For the induced inflow distribution on the rotor disk, the constant vorticity contour wake model is included. For calculating the airloads of two dimensional airfoil with trailing edge flap, the unsteady aerodynamic model of Leishman (Ref 13-14) including the effect of the trailing edge flap is used. The aeroelastic analysis involving computation of advanced tip structural and trailing edge flap aerodynamic matrices has been implemented by using the computer programme ARMDAS (Advanced Rotorcraft Multidisciplinary Design and Analysis System) developed at Nanjing University of Aeronautics and Astronautics (Ref 17).

Formulation

The rotor comprises a number of advanced geometry flexible blades. Each blade is composed of an arbitrary number of Euler-Bernoulli-beam-type straight segments. The main blade can have an arbitrary precone. All other segments can be arbitrarily configured in space with different sweep and pretwist. The analytical model provides for offsets of blade section tension center, center of mass and aerodynamic center from the elastic axis. An arbitrary number of finite elements can be used to model each segment. For the trailing edge flaps, it is assumed that the flap itself is mass balanced and has negligible moment of inertia so that all mass couplings between flap and blade can be ignored. In addition, the mass of the trailing edge

flap actuator is assumed to be zero.

Equations of motion

The equations of motion are derived using Hamilton's principle

$$\int_{t_1}^{t_2} (\delta U - \delta T - \delta W) dt = 0 \quad (1)$$

where δU , δT and δW are, respectively, the variations in the strain energy, the kinetic energy and the virtual work done by external forces.

For swept-tip blade, the key problems are the computations of the blade kinetic energy, δT , and the virtual work, δW , done by the aerodynamic forces on the blade. The variation in kinetic energy for an elastic beam is derived in the undeformed coordinate system of an elastic blade including tip sweep and pretwist. These are also valid for the straight-tip blade.

It is important for the derivation of kinetic energy of elastic beam to determine the position vector of an arbitrary point in the deformed blade with respect to the inertial reference frame. Consider a typical m-th blade segment. The position vectors of arbitrary point P in the m-th blade segment before and after deformations can be expressed as

$$\vec{r}_b = \sum_{n=0}^{m-1} \vec{e}_{km}^T T_{nm}^T L_n + \vec{e}_{km}^T X_P + \vec{e}_{km}^T Y_P \quad (2)$$

$$\begin{aligned} \vec{r}_b' &= \sum_{n=0}^{m-1} \vec{e}_{km}^T T_{nm}^T L_n + \vec{e}_{km}^T X_P + \vec{e}_{km}^T \delta_P + \vec{e}_{km}^T Y_P \\ &= \vec{e}_{km}^T X_m \end{aligned} \quad (3)$$

where

$$X_P = \{x, 0, 0\}^T$$

$$Y_P = \{0, \eta, \zeta\}^T$$

$$\delta_P = \{u, v, w\}^T$$

$$T_{mn} = T_{nb} \cdot T_{mb}^T$$

\vec{e}_{km}^T represents the undeformed m-th segment coordinates of the k-th blade. T_{mn} represents the transformation matrix relating the undeformed n-th segment coordinates to the undeformed m-th segment

coordinates.

By differentiating the position vector with respect to the nonrotating frame, the velocity of the point P in the local coordinate are obtained. It can be expressed as

$$\vec{V}_b = \vec{e}_{km}^T \dot{X}_m + \vec{\omega}_{km} \times \vec{e}_{km}^T X_m \quad (4)$$

where

$$\vec{\omega}_{km} = \vec{e}_{Hr}^T \Omega_r + \vec{e}_b^T \Omega_b$$

$$\Omega_r = \{0, 0, \Omega\}^T$$

$$\Omega_b = \{\dot{\theta}_p, 0, 0\}^T$$

\vec{e}_{Hr} represents the rotating hub-fixed coordinates system. \vec{e}_b represents the undeformed m-th segment coordinates of the k-th blade. Ω represents the angular velocity of rotor. $\dot{\theta}_p$ represents the angular velocity of blade pitching.

The variation of kinetic energy is expressed as

$$\delta T = \int_0^R \iiint_A \rho \vec{V} \cdot \delta \vec{V} d\eta d\zeta dx \quad (5)$$

where η and ζ denote the position of an arbitrary point along the y-axis and z-axis of the undeformed coordinate system. Substituting the velocity expressions and integrating over the cross section, one obtains the expressions of the variation of kinetic energy.

The virtual work δW can be expressed as:

$$\delta W = \int_0^R (L_u \delta u + L_v \delta v + L_w \delta w + M_\phi \delta \phi) dx \quad (6)$$

where L_u , L_v , L_w and M_ϕ are the external aerodynamic loads distributed along the length of the blade in the axial, lag, flap and torsion directions, respectively.

Aerodynamic loads for the dynamic analysis are calculated using the unsteady aerodynamic model of Leishman (Ref 13-14).

The lift and moment on a two dimensional airfoil with plain trailing edge flap is given as

$$C_N(t) = C_N^i(t) + 2\pi C(k) [\alpha_{qs} + \delta_{qs}] \quad (7)$$

$$C_M(t) = C_M^i(t) + \pi \left(a + \frac{1}{2} \right) C(k) [\alpha_{qs} + \delta_{qs}] + C_M^{qs}(t) \quad (8)$$

where

$$C_N^i(t) = \frac{\pi b \dot{\alpha}}{V} + \frac{b}{V^2} \left[\pi \dot{h} - \pi ab \ddot{\alpha} - VF_4 \dot{\delta} - bF_1 \ddot{\delta} \right] \quad (9)$$

$$C_M^i(t) = -\frac{\pi}{2V^2} \left[\left(\frac{1}{8} + a^2 \right) b^2 \ddot{\alpha} - ab \dot{h} \right] - \frac{1}{2V^2} \left[(F_7 + (e-a)F_1) b^2 \ddot{\delta} \right] \quad (10)$$

$$C_M^{qs}(t) = -\frac{1}{2V^2} \left[\pi V \left(\frac{1}{2} - a \right) b \dot{\alpha} + (F_4 + F_{10}) V^2 \delta + \left(F_1 - F_8 - (e-a)F_4 + \frac{1}{2}F_{11} \right) V b \dot{\delta} \right] \quad (11)$$

$$\alpha_{qs} = \left[\frac{\dot{h}}{V} + \alpha + b \left(\frac{1}{2} - a \right) \frac{\dot{\alpha}}{V} \right] \quad (12)$$

$$\delta_{qs} = \left[\frac{F_{10} \delta}{\pi} + \frac{bF_{11} \dot{\delta}}{2\pi V} \right] \quad (13)$$

Note that in these expressions the F terms are geomtric constants that depend only on the size of the flap relative to the airfoil chord (details in Ref 14).

For the calculation of the blade airloads, the information about the wind velocity seen by a blade is required. The resultant velocity seen at a blade section consists of the incoming velocity, the blade motion, and the induced inflow. It can be expressed as

$$\vec{V}_s = \vec{e}_{km}^T \dot{X}_m + \vec{\omega}_{km} \times \vec{e}_{km}^T X_m - \vec{e}_{km}^T V_w \quad (14)$$

where

$$V_w = \{ \mu \Omega R, 0, \lambda \Omega R \}^T \quad (15)$$

$$\lambda = \mu g \alpha_s + \lambda_i \quad (16)$$

μ is the rotor advance ratio, α_s is the attack angle of rotor disk, R is the rotor radius and λ_i is the nondimensional rotor induced inflow.

Rotor wake modeling

For the calculation of the rotor induced inflow, a rotor wake model is required. A simple model is the linear inflow model, such as the Dress model. A complex wake model involves the rotor wake structural analysis. In the present study, a rotor wake modeling using circulation contours is used to calculate the nonuniform inflow distribution on the rotor disk. A new efficient method of constant vorticity contours wake modeling for a helicopter rotor is developed. This method includes three parts: the pre-process of circulation distribution, the determination of generating points of constant vorticity contours and the rotor wake modeling. Compared to the vortex-lattice wake model, the constant vorticity contour wake model has many advantages, such as the reduction of the number of vortex elements and more reasonable distribution of vortex elements as shown in Fig. 1.

Rotor load and response

Under the free flight condition, one can establish six equilibrium equations of the vehicle three force (vertical, longitudinal and lateral), and three moments (pitch, roll and yaw) equations. For a specified weight coefficient C_w and advance ratio μ , the trim solution calculates the attack angles of rotor disk (α_s, ϕ_s), the pitch control settings ($\theta_0, \theta_{1c}, \theta_{1s}$) and the tail rotor thrust. These trim values are recalculated iteratively using the modified rotor hub forces and moments including the blade elastic responses.

The blade loads in rotating frame (i.e. shear forces and bending /torsion moments) are calculated using the force summation method. In this approach, blade aerodynamic and inertia forces are directly integrated over the length of the blade. The hub loads in fixed frame are calculated by summing the contributions from individual blades.

The steady response involves the determination of time dependent blade positions at different azimuth locations for one rotor revolution. To reduce computational time, the finite element equations are transformed into normal mode equations based on the coupled natural modes of the blade.

These nonlinear periodic coupled equations are solved for steady response based on using the temporal finite element method. One rotor revolution is discretized into a number of time elements. Lagrangian shape functions are used as the time interpolation functions. Response periodicity conditions are used during the assembly of the time finite element equations. The resulting nonlinear algebraic normal mode equations are solved using a modified Newton method to yield the blade steady response.

Results and Discussion

Numerical results are calculated for an advance geometry four-bladed, soft-inplane hingeless rotor with Lock number $\gamma = 5.2$, solidity ratio $\sigma = 0.07$, thrust level $C_w = 0.005$, blade aspect ratio $c/R = 0.055$, swept tip length $l_{tip} = 0.08R$, linear pretwist $\theta_{tw} = -5^\circ$ and zero precone. The trailing edge flap is of 20% blade chord and extended from 80-90% blade radius. It is assumed that the effect of the gap between the trailing edge of the blade and the leading edge of the flap is neglected. The chordwise locations of blade center of gravity, aerodynamic center, and tensile axis from the elastic axis are assumed to be zero. The fuselage center of gravity lies on the shaft axis and is located at a distance $0.2R$ below the rotor hub center. The fuselage drag coefficient in terms of flat plate area, i.e., $f/\pi R^2$ is taken as 0.01. The structural properties of the blade are assumed uniform and taken from Ref 17. For the analysis, the blade is discretized into six beam elements and one element presents swept tip. To reduce the computational time, the first six coupled rotating natural modes (three flap, two lag and one torsional modes) are used. For the periodic steady response of the rotor, one cycle of time is discretized into six time elements and each time element is described by a quartic Lagrange polynomial distribution along the azimuth. The first flap, lag, and torsional frequencies are 1.15/rev, 0.74/rev, and 4.45/rev, respectively. The numerical results are calculated for different wake models, tip sweep angles and open loop flap inputs.

Figure 2 shows the calculated inflow distributions with

different wake models. Predicted results with nonuniform inflow model show considerable variations of the induced inflow distribution at the azimuth angle 90 degree and 270 degree.

Figure 3 to figure 5 present the calculated steady tip response for one cycle. Predicted results with different tip sweep angles show considerable effects of tip sweep on blade steady aeroelastic response.

Figure 3 shows that the flap deflection decreases somewhere with increasing sweep angle.

Figure 4 shows the blade lag deflection at tip with azimuth. It is observed that only the steady component of the lag response decreases with tip sweep and the vibratory part is less unaffected. This is due to the kinematic axial-lag coupling and the straightening effect of centrifugal force.

Figure 5 shows considerable effect of tip sweep on the torsional response. This is caused perhaps by an increase of torsional moment with sweep due to an after shift of the aerodynamic center at the tip from the blade elastic axis.

Figure 6 shows the vertical shear load at blade root for two different models. It is shown that the effects of the prescribed wake model on the vertical shear load are quite large as compared to those of the linear inflow model (Dress model).

For the low speed flight condition, it is concluded that the prescribed wake model plays an important role as compared to the linear inflow model. It is also observed that the discrepancy in calculated results between two inflow models is more distinct in load prediction than in blade response.

The rotor transmits the harmonic components from the rotating frame to the nonrotating frame in the form of hub loads. For a four-bladed rotor, the transmitted hub loads consist primarily of 4/rev harmonics in the nonrotating frame. Figure 7 presents the calculated 4/rev vertical hub load variation with advance ratio for different tip sweep angles. It is shown that the swept-tip blade can reduce the 4/rev vertical hub load for most advance ratios. It is also observed that there is a peak of load distribution in low speed region. Because the rotor wake plays an important role for low speed flight condition.

Figure 8 shows the effects of tip sweep on the vertical

shear load at blade root in the rotating frame. It is shown that the effects of tip sweep on the blade root load are not large as compared to the sweep effects on the vertical hub load in nonrotating frame.

Figure 9 shows the effects of tip sweep on the flap bending moments at blade root in the rotating frame. It is shown that the effects of tip sweep on the flap bending moments at blade root are large. The difference in results between the straight tip and the swept-tip may be caused by the change in the effective angle of attack distribution due to sweep.

Figure 10 shows the nondimensional response of the blade tip with the trailing edge flap $+1.5^\circ / -1.5^\circ$ 4/rev input. It is shown that there is a large increase in blade torsional response as compared to the baseline blade. The other responses, flap bending and lag bending, appear to be relatively unaffected by the trailing edge flap input. It appears that vibration reductions with the plain trailing edge flap are more closely associated with changes in blade torsional response than with changes in blade flap or lag bending response.

Conclusions

The effects of different wake models, tip sweep angles and trailing edge flap inputs on rotor blade response and loads have been investigated. Results were obtained for level flight conditions. The following conclusions are drawn from this investigation:

1. For a low speed flight condition, the rotor wake analysis is important for capturing the harmonics of vertical hub loads, flap bending moments and low speed aerodynamic loadings. Using a refined wake model helps to improve the accuracy of aerodynamic calculation.
2. The advanced tips introduce significant effects on the blade steady aeroelastic response. The swept tip increases the vibratory component of torsional response, and thus increases the blade torsional vibratory loads.
3. The swept-tip blade can reduce the 4/rev vertical hub load for most advance ratios. The effects of tip sweep on the blade structural bending moments are quite large for a high speed flight

condition.

4. The trailing edge flap inputs introduce considerable increase of the blade torsional response as compared to the baseline blade. The vibration reductions with the plain trailing edge flap are more closely associated with changes in blade torsional response than with changes in blade flap or lag bending response.

References

1. Desopper A. "Study of unsteady transonic flow on rotor blade with different tip shapes" . *Vertica*, Vol. 9, No. 3, 1985.
2. Desopper A., Lafon P., et al. "Ten years of rotor flows studies at ONERA-State of the art and future studies" , *Proceedings of 42nd Annual Forum of the American Helicopter Society*, Washington, D.C., 1986
3. Celi R., Friedmann P. P. "Aeroelastic modeling of swept tip rotor blades using finite elements," *Journal of the American Helicopter Society*, Vol. 33, No. 2, 1988.
4. Benguet P. Chopra I., "Calculated dynamic response and loads for an advanced tip rotor in forward flight" . *Proceedings of 15th European Rotorcraft Forum*, 1989
5. Kim K.C., Chopra I., "Aeroelastic analysis of helicopter rotor blades with advanced tip shapes" , *Proceedings of 31st AIAA/ ASME / ASCE / AHS / ASC Structures, Structural Dynamics and Materials Conference*, 1990
6. Bir G.S., Chopra I., "Aeromechanical stability of rotorcraft with advanced geometry blades" , *Proceedings of 34th AIAA/ASME/ASCE/AHS/ ASC Structures , Structural Dynamics and Materials Conference*, 1993
7. Spangler, R. L. and Hall, S. R., "Piezoelectric Actuators for Helicopter Rotor Control, " *Proceedings of 31st AIAA/ASME/ASCE/AHS/ ASC Structures , Structural Dynamics and Materials Conference*, AIAA-90-1076-CP, 1990.
8. Walz, C. and Chopra, I. "Design and Testing of a Helicopter Rotor Model with Smart Trailing Edge Flaps," *Proceedings of 35th AIAA/ASME/*

- ASCE/AHS/ASC Structures , Structural Dynamics and Materials Conference, AIAA-94-1767-CP, 1994.*
9. Milgram, J. and Chopra, I., " Helicopter Vibration Reduction with Trailing Edge Flaps," *Proceedings of 36th AIAA/ASME/ASCE/AHS/ASC Structures , Structural Dynamics and Materials Conference, AIAA-95-1227-CP, 1995.*
 10. Millott, T. A. and Friedmann, P. P., "Vibration Reduction in Helicopter Rotors Using an Active Control Surface Located on the Blade, " *Proceedings of 33rd AIAA/ASME/ASCE/AHS/ASC Structures , Structural Dynamics and Materials Conference, AIAA-92-2451-CP, 1992.*
 11. Millott, T. A. and Friedmann, P. P., " The Practical Implementation of an Actively Controlled Flap to Reduce Vibration in Helicopter Rotors," *Proceedings of the 49th Annual Forum of the American Helicopter Society, St. Luis, May 1993, pp. 1079-1092.*
 12. Millott, T. A. and Friedmann, P. P., "Vibration Reduction in Hingless Rotors Using an Actively Controlled Trailing Edge Flap: Implementation and Time Domain Simulation," , *Proceedings of 35th AIAA/ASME/ASCE/AHS/ASC Structures, Structural Dynamics and Materials Conference, AIAA-94-1306-CP, 1994.*
 13. Leishman, J. G., "Unsteady Lift of a Flapped Airfoil by Indicial Concepts," *Journal of aircraft, Vol. 31, No. 2, 1994, pp. 288-297.*
 14. Hariharan N. and Leishman J. G., "Unsteady Aerodynamics of a Flapped Airfoil in Subsonic Flow by Indicial Concepts," *Proceedings of 36th AIAA/ASME/ASCE/AHS/ASC Structures, Structural Dynamics and Materials Conference, AIAA-95-1228-CP, 1995.*
 15. Lou W. J. and Wang S. C., " An Advanced Method for Representing the Helicopter Rotor Wake" . *Proceedings of the 1st Annual Forum of Russian Helicopter Society, Moscow, Russia. 1994.*
 16. Yang W. D., Zhu D.M., " A coupled rotor aeroelastic analysis with swept tips utilizing constant vorticity contour wake model " . *Proceedings of International Conference on Structural Dynamics, Vibration, Noise and Control, Hong Kong, Vol. 1, 1995, pp. 448-453.*
 17. Yang W. D., " Aeroelastic Analysis and Optimization of Helicopter Rotor Blade with Advanced Tips" , *Ph.D. Dissertation, Research Institute of Helicopter Technology, Nanjing University of Aeronautics and Astronautics, 1995.*

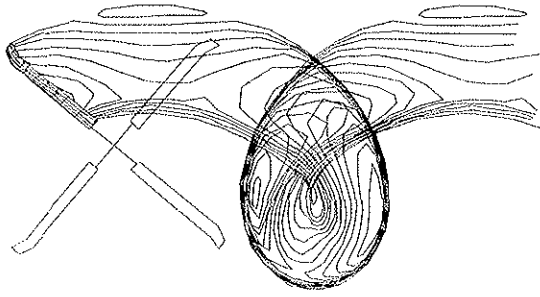


Fig. 1 one blade wake geometry for a four-bladed rotor at advanced ratio 0.30 top view.

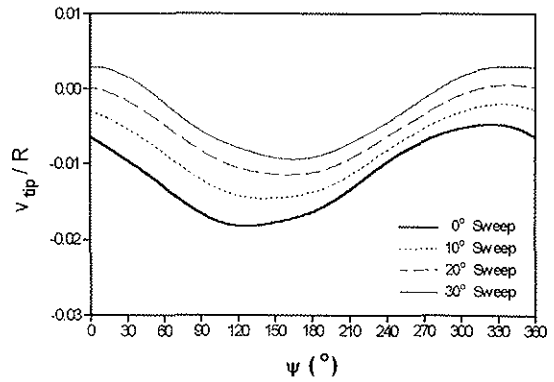


Fig. 4 Effects of tip sweep on lag response at blade tip. ($\mu = 0.3$)

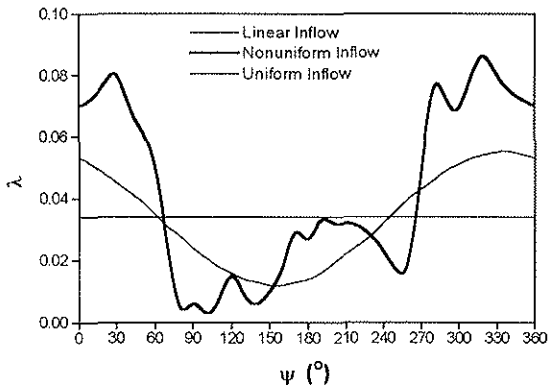


Fig. 2 Effects of wake model on inflow distributions. ($\mu = 0.25$)

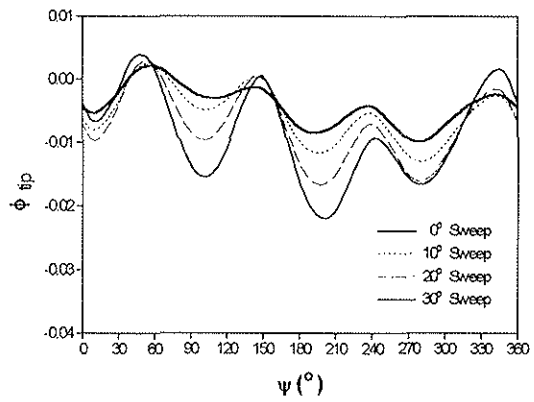


Fig. 5 Effects of tip sweep on torsional response at blade tip. ($\mu = 0.3$)

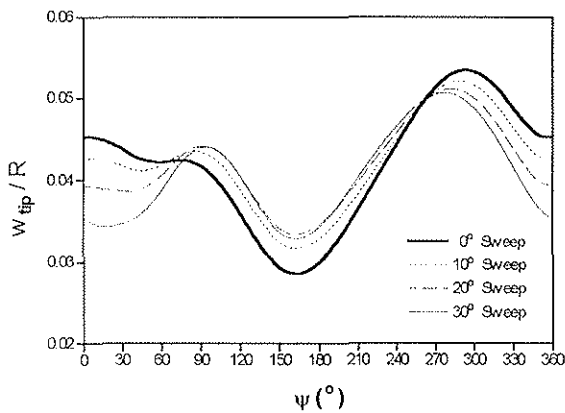


Fig. 3 Effects of tip sweep on flap response at blade tip. ($\mu = 0.3$)

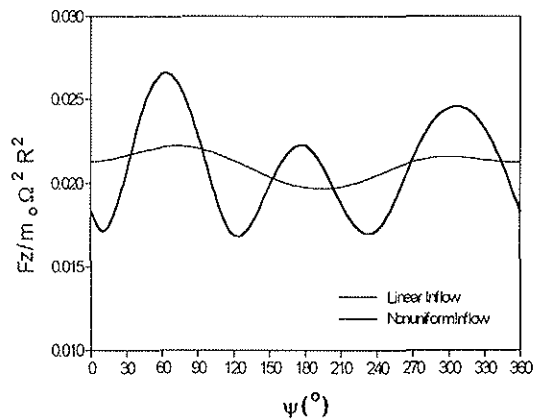


Fig. 6 Effects of wake model on vertical shear at blade root. ($\mu = 0.1$)

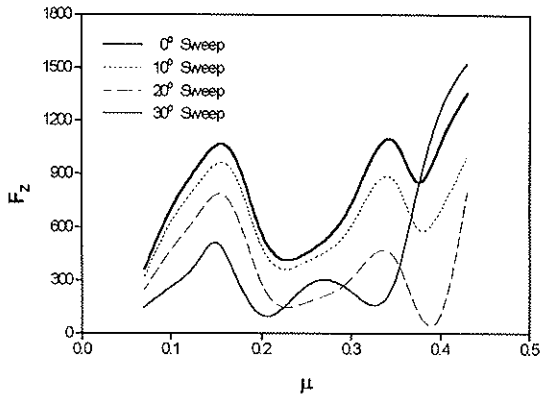


Fig. 7 Effects of tip sweep on 4/rev vertical hub load.

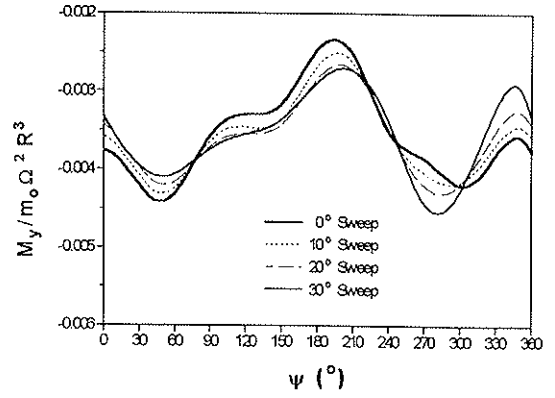


Fig. 9 Effects of tip sweep on flap bending moments at blade root. ($\mu = 0.3$)

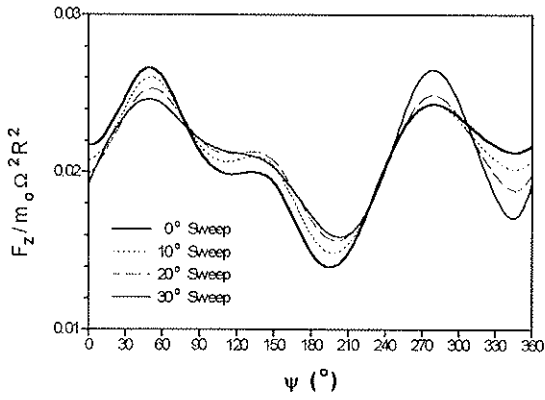


Fig. 8 Effects of tip sweep on vertical shear at blade root. ($\mu = 0.3$)

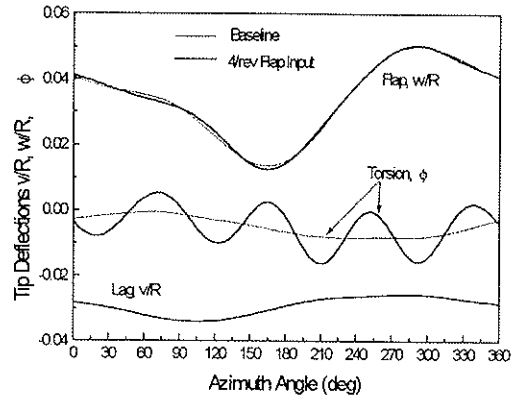


Fig. 10 Effects of flap input on blade response at tip ($\mu = 0.3$)